THE JOURNAL OF
PHYSICAL CHEMISTRY C

Article

pubs.acs.org/JPCC

Surface Charge Transfer Doping of III–V Nanostructures

Kuniharu Takei,[†,‡,§] Rehan Kapadia,[†,‡,§] Yongjun Li,[†] E. Plis,[∥] Sanjay Krishna,[∥] and Ali Javey*[,†,‡,§]

[†]Electrical Engineering and Computer Sciences, and [‡]Berkeley Sensor and Actuator Center, University of California, Berkeley, California 94720, United States

[§]Materials Sciences Division, Lawrence Berkeley National Laboratory, Berkeley, California 94720, United States

[∥]Electrical and Computer Engineering, University of New Mexico, Albuquerque, New Mexico 87106, United States

ABSTRACT: Surface charge transfer is presented as an effective doping technique for III–V nanostructures. We generalize that the technique is applicable to nanoscale semiconductors in the limit where carriers are quantum confined. As a proof-of-concept, potassium surface charge transfer doping is carried out for one-dimensional (1D) and two-dimensional (2D) InAs on Si/SiO_2 substrates. Experiments and simulations show that equivalent dopant areal dose of up to ~2×10^{12} cm^{-2} is obtained, which is sufficient for degenerate doping of InAs nanostructures. This work presents a new pathway for controllable doping of inorganic semiconductors with limits fundamentally different from those of substitutional doping.

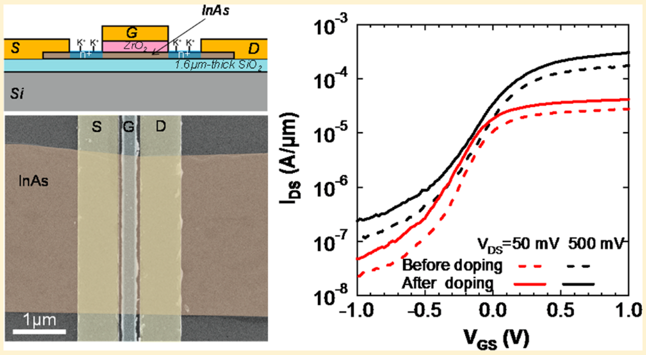

In recent years, III–V semiconductors have been intensively explored for future energy efficient electronics, in part due to their high mobility and saturation velocity as compared to Si.[1−8] For planar field-effect transistors (FETs), a general rule of thumb dictates that to obtain effective gate electrostatic coupling of the channel, a body (i.e., channel) thickness of <1/3 of the channel length should be used to minimize the short channel effects. This suggests that for sub-10 nm channel length devices, the semiconductor thickness should be <3 nm. At this thickness, the carriers in most semiconductors are heavily quantized by the structural confinement effects. This is particularly true for III–V compound semiconductors, which have large excitonic Bohr radii (e.g., InAs Bohr radius is $a_{Bohr} \approx 32$ nm).[1,9] At this extreme scaling limit, new challenges and opportunities arise given the strong quantum confinement of carriers and the molecular-scale dimensions (at least in thickness) of the semiconductors. An example includes uniform and controllable doping. When the thickness is reduced to sub 3-nm, the number of dopant atoms needed per unit area even for high doping concentrations becomes very small, thereby causing large stochastic variation. More importantly, ion implantation is not compatible with nanoscale III–V compound semiconductors because it causes severe structural damage that cannot be perfectly fixed by a subsequent thermal anneal.[10,11] To address this challenge, new doping techniques are needed. In one approach, we recently demonstrated monolayer doping (MLD) of semiconductors as a platform for enabling nanoscale substitutional doping in Si[12,13] and III–V[14,15] structures. The concept relies on the formation of self-limiting molecular monolayers containing dopant species on the surface of semiconductors first, followed by their diffusion into the lattice by a subsequent thermal annealing process. MLD has been shown to be highly versatile and promising as compared to conventional ion implantation doping, enabling extremely shallow doping profiles, down to a few nanometers without structural defects. However, although better than ion implantation, this technique is still based on substitutional doping and diffusion of dopants, and hence at the ultrascaled miniaturization limit, it also suffers from stochastic variation.

Previously, surface charge transfer doping of molecular systems, such as polymers, carbon nanotubes, graphene, and layered chalcogenides, was demonstrated as an effective path for controlling the carrier concentrations.[16−19] As a guideline, doping occurs when the surface dopant, which is often an atom or a molecule, is preferentially oxidized (n-doping) or reduced (p-doping) by the semiconductor. Specifically, n-doping occurs when the highest occupied orbital is above both (i) the lowest conduction subband edge and (ii) the Fermi level in the semiconductor, and p-doping occurs when the lowest unoccupied orbital is both (i) below the highest valence subband edge and (ii) the Fermi level in the semiconductor. However, attempts to use surface charge transfer doping with conventional inorganic semiconductors have largely failed, or resulted in only minimal observed effects.[20] Here, by using InAs nanomembranes (2D) and nanowires (1D) as prototypical material systems, we demonstrate for the first time that surface charge transfer doping can also be highly effective in conventional inorganic semiconductors within a certain constraint. Specifically, as long as the carriers are structurally quantum confined, strong modulation of carrier concentration

Received: June 22, 2013
Revised: July 30, 2013
Published: July 31, 2013

dx.doi.org/10.1021/jp406174r | *J. Phys. Chem. C* 2013, 117, 17845−17849

across the entire body thickness of the semiconductor can be obtained. Given the large Bohr radii of III−V compound semiconductors, this corresponds to structures with dimensions that are readily attainable (i.e., sub-20 nm). The proposed technique is a chemical surface charge doping mediated via deposition of an ionic atom or molecule on a semiconductor surface without high-temperature dopant diffusion. In addition, the doping concentration can be controlled by the quantity of ionic material deposited onto the semiconductor material and the corresponding charge transfer yield, and is not limited by solid solubility limit or defect formation as is the case for substitutional doping. Here, we use potassium, which has one of the lowest ionization energies, as a proof-of-concept surface dopant to effectively tune the electron concentration in InAs nanostructures.

The material and device process scheme is briefly as follows. As previously reported elsewhere,[1] ultrathin InAs membranes (5, 8, and 13 nm thickness) were layer transferred onto Si/SiO_2 substrates from epitaxially grown source substrates. InAs nanowires (NWs) were grown by using a vapor−liquid−solid method with Ni catalysts described previously[21] and drop-casted onto Si/SiO_2 substrates. Both back-gated and top-gated devices were fabricated for doping experiments. For the back-gated device geometry, both 1D and 2D InAs FETs were fabricated on p+Si/SiO_2 (50 nm in thickness) substrates as depicted in Figure 1a. Top-gated devices were fabricated with 2D InAs membranes (Figure 1b). Top-gate stacks of ZrO_2 (∼15 nm)/Ni were underlapped with source (S) and drain (D) metal electrodes, with a gate length of $L_G \approx 200$ nm and S/D spacing $L_{SD} \approx 400$ nm (∼100 nm underlaped for each S/D electrode) as shown in Figure 1b and c. The gate stacks were fabricated with a lift-off process with the underlapped regions allowing for subsequent surface charge transfer doping of InAs in the vicinity of the contacts with the gate serving as a self-aligned mask. For all devices, thermal annealing of Ni S/D contacts in N_2 at 300 and 185 °C for InAs membranes and NWs, respectively, was carried out to achieve low contact resistances as previously reported.[9,22] The devices were mounted on a chip carrier and wire bonded. The samples were loaded in a vacuum chamber with a base pressure of ∼1.5 × 10^{-5} Torr. Potassium was evaporated from a dispenser (SAES Advanced Technologies S.p.A) under vacuum by applying 5A of current for 1 h. Deposition of potassium on the exposed regions of InAs results in electron injection into the semiconductor, realizing n^+ InAs as highlighted in Figure 1a and b. All electrical measurements were performed in situ, without breaking vacuum.

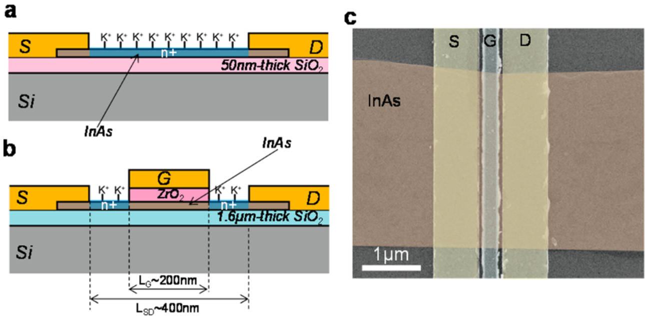

Figure 1. Schematics of (a) back-gated and (b) top-gated InAs FETs used for K surface doping experiments. (c) Representative scanning electron microscopy (SEM) image of a top-gated 2D InAs FET.

First, the maximum doping concentration attainable by potassium vapor deposition was explored as a function of InAs thickness for 2D membranes. Back-gated InAs FETs (channel length ∼5−7 μm) were used to observe the effect of potassium surface charge transfer doping. Figure 2 shows the $I_{DS}-V_{GS}$ characteristics before and after potassium doping for three different membrane thicknesses (T_{InAs} = 5, 8, and 13 nm). A clear shift toward the more negative voltage is observed in the threshold voltage for all three InAs thicknesses after potassium exposure. To determine the effective doping level after K exposure, a two-dimensional Poisson and drift-diffusion simulation was carried out using TCAD Sentaurus2010. In this simulation, the injected electrons from potassium into InAs were modeled by an increased body doping level. Potassium ions on the surface were modeled as an interface fixed charge. An intrinsic (i.e., before potassium doping) body electron concentration of 4 × 10^{16} cm^{-3} was assumed for all three thicknesses, while different interface trap densities (D_{it} = 6 × 10^{12}, 4 × 10^{12}, and 1 × 10^{13} states/cm^2 eV for 5, 8, and 13 nm thick InAs, respectively) were used to fit experimental subthreshold swing before potassium doping. The mobility and series resistance used in the simulation were those extracted from experiments. An electron effective mass of $0.023m_0$, where m_0 is the electron rest mass in vacuum, was used for all thicknesses because the error due to the change in effective mass versus confinement is negligible in the range of the thickness explored here. Bandgaps of 0.54, 0.45, and 0.4 eV were used for the 5, 8, and 13 nm thick InAs, respectively, with the quantum confinement effects obtained from k.p. calculation

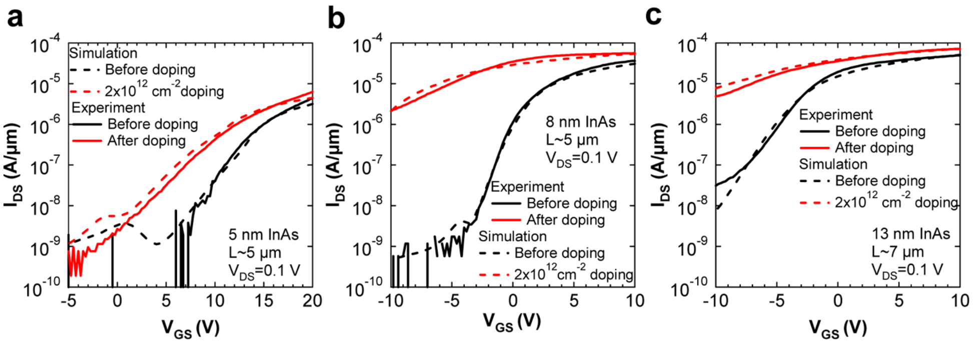

Figure 2. Electrical characteristics of back-gated InAs FETs at V_{DS} = 0.1 V with different membrane thickness of (a) 5 nm ($L_{SD} \approx 5$ μm), (b) 8 nm ($L_{SD} \approx 5$ μm), and (c) 13 nm ($L_{SD} \approx 7$ μm) before (black) and after (red) surface charge doping with potassium. Solid lines and dash lines represent experiments and modeling, respectively.

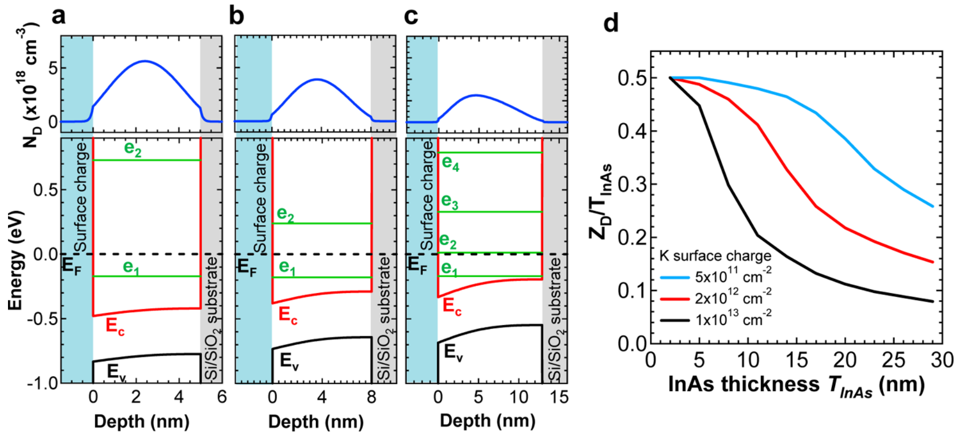

Figure 3. Calculated charge density profiles and band diagrams of back-gated InAs membranes. (a) 5 nm, (b) 8 nm, and (c) 13 nm thick InAs membranes. e1−e4 correspond to the edge of four lowest electron subbands. (d) Calculated charge centroid normalized by InAs thickness (Z_d/T_{InAs}) as a function of InAs thickness and surface charge. $Z_d/T_{InAs} \approx 0.5$ indicates that the charge centroid is in the middle of InAs body.

incorporated in the simulation. The surface charge concentration needed to fit the experimental electrical characteristics after doping was $n \approx 2 \times 10^{12}$ cm^{-2} for all InAs thicknesses explored here. In the simulation, this charge is assumed to be uniform across the channel. This corresponds to the dopant areal dose obtained with K doping, and the fact that the value is the same for all three thicknesses suggests that the surface charge doping is reproducible and consistent. Clearly, a good fit between experiments and modeling is obtained for all thicknesses, suggesting the accuracy of the extracted dopant dose. Assuming a potassium monolayer surface coverage of ~5 × 10^{14} atoms/cm^2, a charge transfer yield of ~1% is obtained from the experimentally extracted sheet electron density. It should be noted that based on our previous study,[1] 1−2 nm thick native oxide exists on the surface of InAs, which affects the charge transfer yield. InAs surface treatment effects should be further studied in the future to explore the limits of surface charge transfer doping by K. Nevertheless, the obtained electron sheet density is high enough to degenerately dope InAs, especially for thinner membranes.

To further shed light on the effect of surface charge injection as a function of InAs thickness, the charge (i.e., electron) density profile along the thickness of InAs was simulated at a fixed back-gate voltage of 0 V and dopant areal dose of 2 × 10^{12} cm^{-2} (Figure 3a−c). The energy band diagrams and quantum confined electron densities were simulated by solving the Schrodinger−Poisson equation. Because the surface charge density due to potassium is constant ($n = 2 \times 10^{12}$ cm^{-2}), the charge concentration in the body, N_D ($=n/T_{InAs}$) has a thickness dependence. Importantly, the charge centroid Z_d for the first subband (e1) is nearly in the middle of the body ($Z_d/T_{InAs} \approx 0.5$) for 5 and 8 nm thick InAs membranes after surface charge injection. This $Z_d/T_{InAs} \approx 0.5$ indicates that the surface charge injection dopes the entire body effectively as if the doping was induced substitutionally. However, the charge centroid for 13 nm thick InAs is shifted closer to the top surface, suggesting that the potassium more effectively dopes the surface for this thicker membrane. The charge centroid was calculated with different surface charge of potassium ((0.5−10) × 10^{12} cm^{-2}) and InAs thickness ranging from 2 to 29 nm as shown in Figure 3d. As depicted in Figure 3d, the charge centroid depends on both the thickness and the dopant areal dose. Overall, sub-10 nm thickness results in Z_d/T_{InAs} of ~0.4−0.5 for the explored dose. Note that for thicker InAs membranes, surface charge transfer doping still works; however, one obtains higher carrier concentrations near the surface as opposed to the rest of the body, which may be desirable for certain device structures. The simulation result suggests that surface charge transfer doping can be highly effective in tuning the carrier concentrations of nanoscale III−V materials as was experimentally evident in Figure 2. While these calculations are specific to InAs, the result is general and holds for any material system when the material thickness is ~1/3 × a_{Bohr}, corresponding to the regime where carriers are strongly quantum confined.

The chemical surface charge transfer doping can be adapted to a wide range of III−V nanostructures. For instance, 1D InAs NWs were also used to explore this doping concept (Figure 4).

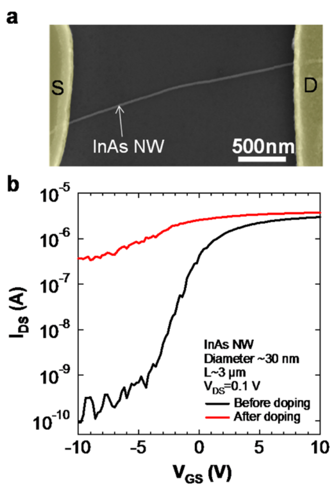

Figure 4. Surface doping of back-gated InAs NW FETs. (a) SEM image of a representative InAs NW FET. (b) I_{DS}−V_{GS} characteristics at V_{DS} = 0.1 V before (black) and after (red) potassium surface exposure.

A back-gated device geometry (Figure 4a) was utilized with a NW diameter of ~30 nm. Figure 4b exhibits the I_{DS}−V_{GS} characteristics before and after potassium surface doping. After doping, off-current at V_{GS} = −10 V clearly increases by ~3 orders of magnitude due to the electron injection from potassium and positive charge of potassium on InAs surface. The result is qualitatively similar to that of InAs membranes shown in Figure 2.

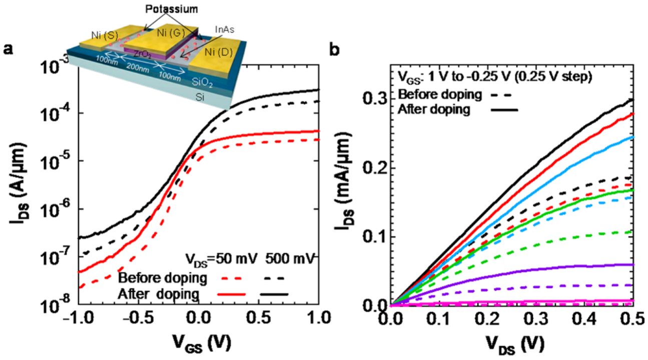

Figure 5. Top-gated InAs FETs with self-aligned, surface-doped S/D contacts based on 8 nm thick InAs membranes. (a) $I_{DS}-V_{GS}$ characteristics at V_{DS} = 50 and 500 mV before (dashed lines) and after (solid lines) K doping of the contacts. (b) $I_{DS}-V_{DS}$ characteristics with V_{GS} from 1 to −0.25 V (0.25 V step). Solid lines and dash lines represent after and before K doping of the contacts, respectively.

Surface charge transfer doping can be readily adopted to fabricate FETs with electron doped S/D contacts that are self-aligned in respect to the gate electrode. To demonstrate this concept, top-gated FETs with a gate length of $L_G \approx 200$ nm and underlapped regions of ∼100 nm on each side of the metal contacts (i.e., $L_{SD} \approx 400$ nm) were fabricated. An 8 nm-thick InAs membrane was used as the channel on a 1.6 μm-thick SiO_2/p+Si substrate. Figure 5a and b shows $I_{DS}-V_{GS}$ and $I_{DS}-V_{DS}$ characteristics before and after potassium doping. A back gate bias of 40 V was applied to the Si substrate to cause accumulation in the underlapped InAs regions. Notably, the on-current at V_{DS} = 0.5 V and V_{GS} = 1 V increases by about 50% after potassium doping. Transconductance, g_m, is ∼0.41 mS/μm after doping as compared to ∼0.26 mS/μm before doping. This improvement by K doping is due to two reasons: (1) lower series resistance of the underlapped InAs regions and (2) lower quantum contact resistance for S/D contacts.[9] Specifically, contact resistance for 8 nm thick InAs membrane extracted experimentally by using a transfer length method[9] is decreased by ∼9% after K doping. The results clearly demonstrate the effective use of surface charge transfer doping for III−V device applications.

In summary, surface charge transfer doping is demonstrated as an alternative pathway to conventional substutional doping for tuning the electron concentration of 2D and 1D InAs nanostructures. Potassium, which is known for its electron-donating attributes, was used as a proof-of-concept surface charge transfer dopant. This surface doping technique does not utilize high temperature processing or dopant diffusion, and thereby in principle reduces stoichiastic dopant variation, which is a fundamental challenge facing future scaled devices. Through experiments and modeling, it is shown that surface charge injection results in the effective "doping" of the entire body of a semiconductor in the limit where the carriers are quantum confined. Given that all future electronic devices require the use of semiconductors with sub-10 nm dimensions, where quantum confinement effects are strong, the surface charge transfer presents a highly viable doping route. In the future, the same scheme may be adopted for hole doping by using molecules with lowest unoccupied molecular obritals below both the valence band edge and the Fermi level of the semiconductor. A variety of electron-withdrawing and -donating molecules and materials with high air stability need to be explored for both p- and n-type doping. In addition, detailed atomistic modeling of the surface charge injection process is needed to shed light on the ultimate limit of the carrier sheet densities that can be obtained.

■ AUTHOR INFORMATION

Corresponding Author

*E-mail: ajavey@eecs.berkeley.edu.

Notes

The authors declare no competing financial interest.

■ ACKNOWLEDGMENTS

The materials processing and characterization of this work were supported by the Director, Office of Science, Office of Basic Energy Sciences, Materials Sciences and Engineering Division, of the U.S. Department of Energy under contract no. DE-AC01-05CH11231. The device fabrication was supported by NSF E3S Center. A.J. acknowledges support from the World Class University program at Sunchon National University.

■ REFERENCES

(1) Ko, H.; Takei, K.; Kapadia, R.; Chuang, S.; Fang, H.; Leu, P. W.; Ganapathi, K.; Plis, E.; Kim, H. S; Chen, S.-Y.; et al. Ultrahin Compound Semiconductor on Insulator Layers for High Performance Nanoscale Transistors. *Nature* **2010**, *468*, 286−289.

(2) del Alamo, J. A. Nanometre-scale Electronics with III-V Compound Semiconductors. *Nature* **2011**, *479*, 317−323.

(3) Kim, D.-H.; del Alamo, J. A. Scalability of Sub-100 nm InAs HEMTs on InP Substrate for Future Logic Applications. *IEEE Trans. Electron Devices* **2010**, *57*, 1504−1511.

(4) Yokoyama, M.; Iida, R.; Kim, S. H.; Taoka, N.; Urabe, Y.; Yasuda, T.; Takagi, H.; Yamada, H.; Fukuhara, N.; Hata, M.; et al. Sub-10-nm Extremely Thin Body InGaAs-on-Insulator MOSFETs on Si Wafers with Ultrathin Al_2O_3 Buried Oxide Layers. *IEEE Electron Device Lett.* **2011**, *32*, 1218−1220.

(5) Radosavljevic, M.; Chu-Kung, B.; Corcoran, S.; Dewey, G.; Hudait, M. K.; Fastenau, J. M.; Kavalieros, J.; Liu, W. K.; Lubyshev, D.; Metz, M.; et al. Advanced High-k Gate Dielectric for High-Performance Short-Channel $In_{0.7}Ga_{0.3}As$ Quantum Well Field Effect Transistors on Silicon Substrate for Low Power Logic Applications. *IEEE Tech. Dig. Int. Electron Devices Mtg.* **2009**, 319.

(6) Bennett, B. R.; Ancona, M. G.; Boos, J. B. Compound Semiconductors for Low-Power p-Channel Field-Effect Transistors. *MRS Bull.* **2009**, *34*, 530−536.

(7) Takei, K.; Madsen, M.; Fang, H.; Kapadia, R.; Chuang, S.; Kim, H. S.; Liu, C.-H.; Plis, E.; Nah, J.; Krishna, S.; et al. Nanoscale InGaSb Heterostructure Membranes on Si Substrates for High Hole Mobility Transistors. *Nano Lett.* **2012**, *12*, 2060−2066.

(8) Xuan, Y.; Wu, Y. Q.; Shen, T.; Yang, T.; Ye, P. D. High Performance Submicron Inversion-Type Enhancement-Mode InGaAs MOSFETs with ALD Al_2O_3, HfO_2, and HfAlO as gate dielectrics. *IEEE Tech. Dig. Int. Electron Device Mtg.* **2007**, 637.

(9) Takei, K.; Fang, H.; Kumar, S. B.; Kapadia, R.; Gao, Q.; Madsen, M.; Kim, H. S.; Liu, C.-H.; Chueh, Y.-L.; Plis, E.; et al. Quantum Confinement Effects in Nanoscale-Thickness InAs Membranes. *Nano Lett.* **2011**, *11*, 5008−5012.

(10) McNally, P. J. Ion Implantation in InAs and InSb. *Radiat. Eff.* **1970**, *6*, 149−153.

(11) Baca, A. G.; Chang, P. C.; Allerman, A. A.; Drummond, T. J. GaAs Self-Aligned JFETs with Carbon-Doped p^+ Region. *Proc. Electrochem. Soc.* **1999**, *99*, 155.

(12) Ho, J. C.; Yerushalmi, R.; Jacobson, Z.; Fan, Z.; Alley, R. L.; Javey, A. Controlled Nanoscale Doping of Semiconductors via Molecular Monolayers. *Nat. Mater.* **2008**, *7*, 62−67.

(13) Ho, J. C.; Yerushalmi, R.; Smith, G.; Majhi, P.; Bennett, J.; Halim, J.; Faifer, V. N.; Javey, A. Wafer-Scale, Sub-5 nm Junction Formation by Monolayer Doping and Conventional Spike Annealing. *Nano Lett.* **2009**, *9*, 725−730.

(14) Ho, J. C.; Ford, A. C.; Chueh, Y.-L.; Leu, P. W.; Ergen, O.; Takei, K.; Smith, G.; Majhi, P.; Bennet, J.; Javey, A. Nanoscale Doping of InAs via Sulfur Monolayers. *Appl. Phys. Lett.* **2009**, *95*, 072108.

(15) Cho, K.; Ruebusch, D. J.; Lee, M. H.; Moon, J. H.; Ford, A. C.; Kapadia, R.; Takei, K.; Ergen, O.; Javey, A. Molecular Monolayers for Conformal, Nanoscale Doping of InP Nanopillar Photovoltaics. *Appl. Phys. Lett.* **2011**, *98*, 203101.

(16) Kong, J.; Zhou, C.; Yenilmez, E.; Dai, H. Alkaline Metal-Doped n-type Semiconducting Nanotubes as Quantum Dots. *Appl. Phys. Lett.* **2000**, *77*, 3977.

(17) Javey, A.; Tu, R.; Farmer, D. B.; Guo, J.; Gordon, R. G.; Dai, H. High Performance Nanotube n-FETs with Chemically Doped Contacts. *Nano Lett.* **2005**, *5*, 345−348.

(18) Ohta, T.; Bostwick, A.; Seyller, T.; Horn, K.; Rotenberg, E. Controlling the Electronic Structure of Bilayer Graphene. *Science* **2006**, *313*, 951−954.

(19) Fang, H.; Tosun, M.; Seol, G.; Chang, T. C.; Takei, K.; Guo, J.; Javey, A. Degenerate n-Doping of Few-Layer Transition Metal Dichalcogendies by Potassium. *Nano Lett.* **2013**, *13*, 1991−1995.

(20) He, T.; Corley, D. A.; Lu, M.; Spigna, N. H. D.; He, J.; Nackashi, D. P.; Franzon, P. D.; Tour, J. M. Controllable Molecular Modulation of Conductivity in Silicon-Based Devices. *J. Am. Chem. Soc.* **2009**, *131*, 10023−10030.

(21) Ford, A. C.; Ho, J. C.; Fan, Z.; Ergen, O.; Altoe, V.; Aloni, S.; Razavi, H.; Javey, A. Synthesis, Contact Printing, and Device Characterization of Ni-Catalyzed, Crystalline InAs Nanowires. *Nano Res.* **2008**, *1*, 32−39.

(22) Chueh, Y.-L.; Ford, A. C.; Ho, J. C.; Jacobson, Z. A.; Fan, Z.; Chen, C.-Y.; Chou, L.-J.; Javey, A. Formation and Characterization of Ni_xInAs/InAs Nanowire Heterostructures by Solid Source Reaction. *Nano Lett.* **2008**, *8*, 4528−4533.